



ELSEVIER

Contents lists available at ScienceDirect

Chinese Chemical Letters

journal homepage: [www.elsevier.com/locate/ccllet](http://www.elsevier.com/locate/ccllet)

# Photo-induced Ag modulating carbon dots: Greatly improved fluorescent properties and derived sensing application

Yuwei Wang<sup>a</sup>, Ye Li<sup>a</sup>, Guixiang Yang<sup>a</sup>, Xiaofeng Yang<sup>b,\*</sup>, Chenglu Yan<sup>c</sup>, Huaqiao Peng<sup>c</sup>, Huiyong Wang<sup>d</sup>, Juan Du<sup>a,\*</sup>, Baozhan Zheng<sup>a,\*</sup>, Yong Guo<sup>a</sup><sup>a</sup> Department of Chemistry, Sichuan University, Chengdu 610064, China<sup>b</sup> Institute of Quality Standard and Testing Technology for Agro-products, Sichuan Academy of Agricultural Sciences, Chengdu 610066, China<sup>c</sup> Key Laboratory of Aviation Fuel & Chemical Airworthiness and Green Development, The Second Research Institute of Civil Aviation Administration of China, Chengdu 610041, China<sup>d</sup> School of Chemistry and Chemical Engineering, Henan Normal University, Xinxiang 453007, China

## ARTICLE INFO

### Article history:

Received 23 December 2022

Revised 24 February 2023

Accepted 28 February 2023

Available online 5 March 2023

### Keywords:

Carbon dots

Photo-induced Ag modulating

Fluorescent enhancement

High quantum yield

Derived sensing application

Sulfide determination

## ABSTRACT

Carbon dots (CDs) have been attracted much attention and widely studied due to their excellent fluorescence (FL) properties, better biocompatibility and outstanding photo/chemical stability. However, the disadvantage of lower quantum yield (QY) still limits its wide application. Herein, we reported a novel and convenient strategy to prepare photo-induced Ag/CDs (p-Ag/CDs) by irradiating the mixed Ag<sup>+</sup> and hydrophobic CDs (h-CDs) acetone solution with ultraviolet (UV) light. The obtained p-Ag/CDs exhibit a greatly enhanced FL emission together with a blue shift (460 nm) than h-CDs (520 nm). The QY of p-Ag/CDs is measured to be 51.1%, which is 10.4 times higher than that of h-CDs (4.9%), indicating that photo-induced Ag modulation can effectively improve the optical properties of CDs. The mechanisms for the FL enhancement and blue shift of h-CDs are studied in detail. The results prove that the greatly enhanced FL emission is from the generated Ag nanoparticles (AgNPs) by UV light irradiation based on metal-enhanced fluorescence (MEF), and the increased oxygen-contained groups in this process lead to the blue shift in CDs fluorescence. Interestingly, the p-Ag/CDs exhibit higher sensitivity and selectivity for sulfide ions (S<sup>2-</sup>) detection than that of h-CDs, which have a lower response to S<sup>2-</sup>. This work not only offers a novel strategy to improve the FL properties of materials but also endows them with new functions and broadens their application fields.

© 2023 Published by Elsevier B.V. on behalf of Chinese Chemical Society and Institute of Materia Medica, Chinese Academy of Medical Sciences.

Carbon dots (CDs), a newcomer in carbon nanomaterials, have attracted extensive attention from researchers since their discovery in 2004 [1]. The main advantages of CDs compared with traditional quantum dots (such as PbS, CdS, CdSe) and organic molecules are their excellent luminescence, outstanding photo/chemical stability, biocompatibility and low cost [2], which leads to the widespread application of CDs in photo/electrocatalysis [3–6], sensing [7–11], light-emitting devices [12–16], medical imaging [17–20] and so on. However, CDs still suffer from the disadvantages of lower quantum yield (QY), a significant parameter to characterize the fluorescent materials, and most of the reported CDs have a QY lower than 20% [21], which severely limits their applications in many fields. Therefore, it is urgent and necessary to develop new strategies to im-

prove the optical properties of CDs, which will certainly expand their new practical applications.

It is reported that the optical properties of CDs can be well improved by regulating their compositions, types of groups on the surface, and the state of the carbon core [22]. Based on these, plenty of techniques have been developed to enhance the fluorescent QY of CDs, including surface passivation [23], functionalization [24–27], heteroatomic doping [28–32] and so on. All these methods can effectively improve the fluorescence (FL) properties of CDs to a certain extent, but there are also some shortcomings. For example, Sun *et al.* [23] enhanced the QYs of CDs from 4% to 10% by surface passivation with polyethylene glycol (PEG), while this process involves high-temperature conditions and a longer reaction time (72 h). Zhao *et al.* [26] increased the relative QYs from 1.65% (lignin-based carbon quantum dots, L-CQDs) to 5.54% (aminated lignin carbon quantum dots, NL-CQDs) and 5.90% (reduced-lignin carbon quantum dots, RL-CQDs) by amination and hydroxylation, respectively. Whereas, it is difficult to form a general strat-

\* Corresponding authors.

E-mail addresses: [yangxiaofeng\\_cd@sina.com](mailto:yangxiaofeng_cd@sina.com) (X. Yang), [dujuanchem@scu.edu.cn](mailto:dujuanchem@scu.edu.cn) (J. Du), [zhengbaozhan@scu.edu.cn](mailto:zhengbaozhan@scu.edu.cn) (B. Zheng).

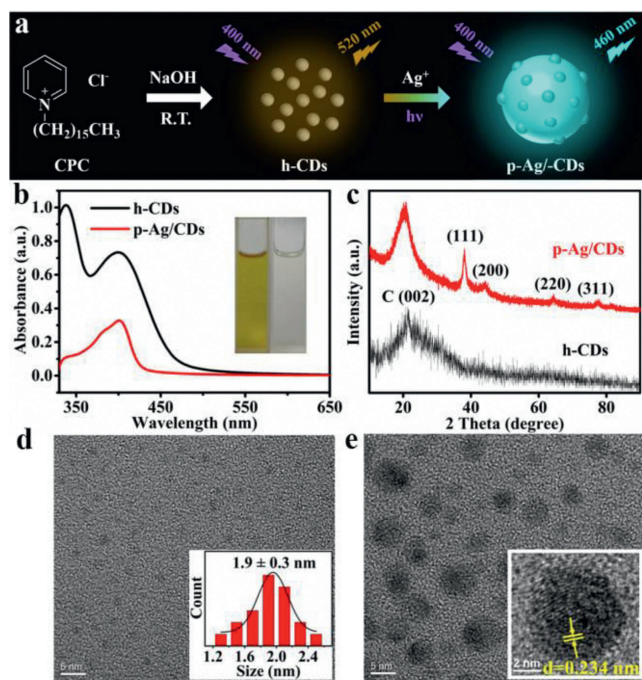


**Fig. 1.** (a) Schematic representation of synthetic routes for p-Ag/CDs. (b) UV-vis absorption spectra of h-CDs and p-Ag/CDs, respectively. [Insets: photos of h-CDs (left) and p-Ag/CDs (right) acetone solution under natural light]. (c) XRD patterns of h-CDs and p-Ag/CDs. (d) TEM image of h-CDs and their size distribution (Inset). (e) TEM and HR-TEM (Inset) images of p-Ag/CDs.

egy due to the complex groups on the CDs surface. Manioudakis *et al.* [28] elevated the QY of  $\text{NH}_3$ -CDs from 1.4% to 33% with nitrogen doping, but this reaction process underwent complicated separation and purification processes, such as dialysis, organic washing and so on. In addition, this improvement is not high enough for its application. These disadvantages all prompt the researchers to develop more efficient and facile methods to synthesize CDs with excellent FL properties. Furthermore, if the materials can be endowed with new derived functions, it will be more beneficial to expand their applications.

Herein, a novel and convenient strategy based on silver modulation was developed to effectively improve the FL properties of CDs. By simple irradiation of  $\text{Ag}^+$  and the hydrophobic carbon dots (h-CDs) acetone solution with ultraviolet (UV) light, photo-induced Ag-modulated CDs (p-Ag/CDs) can be simply synthesized with an obvious blue shift FL emission compared to h-CDs. More important is that the p-Ag/CDs also exhibit a greatly enhanced FL with an absolute QY of 51.1%, which is higher than the original h-CDs (4.9%). The experimental results demonstrate that it is the generated Ag/Ag<sup>+</sup> and increased O-contained groups on the CDs surface by UV irradiation that leads to its FL enhancement and blue shift, respectively. Furthermore, the combination of Ag and CDs also endows p-Ag/CDs with a newly derived FL response to  $\text{S}^{2-}$  compared to original h-CDs. Thus, p-Ag/CDs can be successfully used to construct FL probes for  $\text{S}^{2-}$  detection in real samples with excellent selectivity and accuracy. This work provides a new way to improve the FL properties and new derived functions of CDs, which doubtlessly broadens its applications in many fields.

As shown in Fig. 1a, h-CDs were prepared with cetylpyridinium chloride (CPC) as carbon precursor at room temperature, and its water contact angle was 137°, further indicating that it was a hydrophobic nanomaterial (Fig. S1 in Supporting information). p-Ag/CDs were synthesized by irradiating the mixed  $\text{Ag}^+$  (1 mmol/L) and h-CDs acetone solution with a UV light (365 nm) irradiation time of 22 h (Fig. S2 in Supporting information). Fig. 1b shows the ultraviolet-visible (UV-vis) absorption spectra of h-CDs and ob-

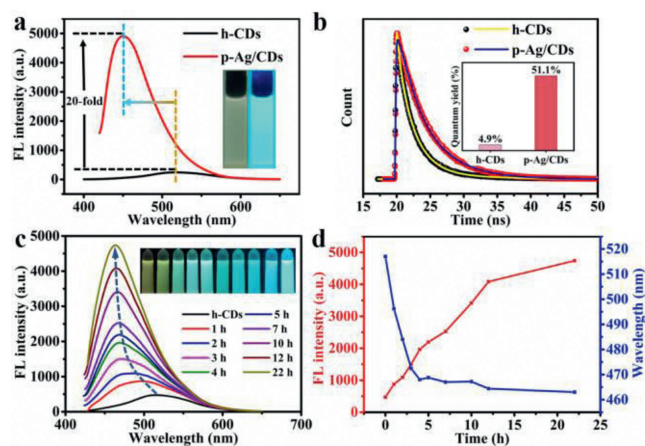


**Fig. 2.** (a) FL spectra of h-CDs and p-Ag/CDs. Insets: photos of h-CDs (left) and p-Ag/CDs (right) solution under the irradiation of UV light (365 nm). (b) Time-resolved FL decay spectra of h-CDs and p-Ag/CDs. Inset: the absolute QY of h-CDs and p-Ag/CDs. (c) FL spectra of h-CDs with the presence of  $\text{Ag}^+$  (1 mmol/L) with different UV light (365 nm, 3 W) irradiation time (0–22 h). Insets: FL photographs of FL spectra corresponding in sequence. (d) The FL intensity and emission wavelength changes of the solutions at different UV light irradiation times.

tained p-Ag/CDs, respectively. From the results, it can be seen that there are two obvious absorption peaks at 340 nm and 400 nm for h-CDs (black line), which should be attributed to the  $\pi \rightarrow \pi^*$  and  $n \rightarrow \pi^*$  transitions, respectively [33]. But for p-Ag/CDs (red line), the absorption peak at 400 nm increases apparently compared to that at 340 nm, and the absorbance ratio of these two peaks ( $A_{400}/A_{340}$ ) was calculated to be 2.29, which is much higher than that of h-CDs (0.72). The increased absorption at 400 nm is attributed to the characteristic surface plasmon resonance (SPR) adsorption of Ag nanoparticles (AgNPs) [34], demonstrating the formation of AgNPs during this irradiation process. The insets of Fig. 1b display the photos of h-CDs and p-Ag/CDs acetone solution under natural light. We can see that the h-CDs solution is yellow (left), while the p-Ag/CDs solution is colorless and transparent (right), which agrees well with the decreased absorbance at 340 nm for p-Ag/CDs compared to h-CDs.

Fig. 1c displays the X-ray diffraction (XRD) patterns of h-CDs and p-Ag/CDs, respectively. The broad diffraction peak at 21.4° belongs to the (002) diffraction of graphene in h-CDs [35]. The four peaks at 38.08°, 44.21°, 64.44° and 77.44° should be from the diffraction of (111), (200), (220) and (311) planes of the face-centered cubic lattice of Ag(0) (JCPDS card No. 04-0783) [36], further indicating the formation of AgNPs during the photo-irradiation process. The transmission electron microscope (TEM) image shown in Fig. 1d exhibits the uniform size of h-CDs with an average size of  $1.9 \pm 0.3$  nm. Fig. 1e shows the TEM image of p-Ag/CDs, in which bigger particles (~6 nm) than h-CDs can be obviously observed. The 0.234 nm lattice fringe spacing obtained from the HR-TEM (Inset of Fig. 1e) is consistent with the (111) plane of face-centered cubic AgNPs [37], which also confirms the formation of AgNPs.

FL is the main characteristic of CDs, so we then studied the FL properties of h-CDs and p-Ag/CDs, especially their FL changes during the photo-irradiation process. Fig. 2a shows the FL spectra of h-CDs and p-Ag/CDs, respectively. As can be seen from the results, p-Ag/CDs exhibit a very strong FL emission (red line), which is about 20 times higher than that of h-CDs (black line). More interesting is that the FL emission of p-Ag/CDs ( $\lambda_{em} = 460$  nm) has a significant 60 nm blue shift compared to that of h-CDs ( $\lambda_{em} = 520$  nm). Insets of Fig. 2a display the FL photos of h-CDs and p-Ag/CDs under UV light irradiation (365 nm). We can see that h-CDs emit a weak yellow FL, while the p-Ag/CDs solution shows a strong blue FL, which

is in good agreement with the FL spectra described above. Furthermore, the FL lifetime of h-CDs and p-Ag/CDs was then investigated, respectively. As shown in Fig. 2b, the average lifetime of p-Ag/CDs was measured to be 4.12 ns, which is higher than that of h-CDs (2.09 ns). The increased lifetime can be explained by the formation of Ag<sup>0</sup> resulting in new electron-transfer processes, which improves the FL property of h-CDs. In addition, the quantum yield (QY) of p-Ag/CDs was also measured and calculated to be 51.1% (Inset of Fig. 2b), which is about 10.4 times higher than that of h-CDs (4.9%), further demonstrating the outstanding FL properties of p-Ag/CDs. In addition, the obtained p-Ag/CDs exhibit excitation-independent FL emission properties (Fig. S3 in Supporting information). The stability of the prepared p-Ag/CDs was then tested. As shown in Fig. S4 (Supporting information), the FL intensity of p-Ag/CDs did not decrease with the continuous irradiation of excitation light (400 nm) for 2 h, proving the excellent photostability of p-Ag/CDs.

To further investigate the effect of Ag<sup>+</sup> and UV light irradiation on the optical properties of h-CDs, the FL spectra of h-CDs with Ag<sup>+</sup> presence were measured at different conditions. From Fig. S5 (Supporting information), we can see that there is no obvious FL enhancement by simply mixing of h-CDs and Ag<sup>+</sup>, demonstrating that the presence of Ag<sup>+</sup> has almost no effect on the FL enhancement of h-CDs. However, the FL intensity of the solution significantly increases with the continuous UV light irradiation for 22 h, and a gradual blue shift of FL emission from 520 nm to 460 nm can be observed at the same time (Fig. 2c). Accordingly, the real-time photos (insets of Fig. 2c) also display the gradually enhanced FL intensity and continuous FL emission changes from weak yellow to strong blue as the increased UV light irradiation time. Fig. 2d exhibits the variation trend of FL intensity and emission wavelength of the solution during the irradiation process. It can be seen that the FL intensity increases linearly within the irradiation time for 12 h, which should be attributed to the gradual increase of Ag<sup>0</sup> during the photo-reaction process. However, the blue shift in FL only occurs in the first 4 h of UV irradiation (Fig. 2d), which, combined with the previous results, suggests that the blue shift in FL may be independent of the produced Ag<sup>0</sup>.

Fourier transfer infrared (FT-IR) and X-photoelectron spectroscopy (XPS) measurements are further carried out to investigate the changes in compositions and groups on h-CDs and p-Ag/CDs. As shown in Fig. 3a, the broad absorption at 3440 cm<sup>-1</sup> should be ascribed to the stretching vibration of O-H/N-H in h-CDs and p-Ag/CDs respectively [38]. The characteristic peaks emerging at 2930 and 2850 cm<sup>-1</sup> are attributed to the stretching vibrations of C-H [39]. These results indicate the co-presence of hydrophilic and lipophilic groups on the surface of h-CDs and p-Ag/CDs. In addition, the peak at about 1660 cm<sup>-1</sup> should be from the stretching vibration of C=O/C=N [40], demonstrating the formation of a conjugated polyaromatic structure on the CDs surface during the reaction [41]. However, the intensity of C=O in p-Ag/CDs is obviously stronger than that in h-CDs (Fig. 3a), together with the stronger absorption at 3440 cm<sup>-1</sup> for p-Ag/CDs, which can prove that there are more oxygen-containing groups in p-Ag/CDs than in h-CDs. Furthermore, the enhanced C-O stretching vibration absorption peak of p-Ag/CDs at 1384 cm<sup>-1</sup> indicates the increased oxygen-containing groups as well [42].

The XPS characterizations of the samples can provide more convincing explanations for the elemental contents and surface groups. As shown in Fig. 3b, the main elements in h-CDs and p-Ag/CDs are C, N and O, but the content of O in p-Ag/CDs (10.25%) is much higher than that in h-CDs (4.79%) (Table S1 in Supporting information), which agrees well with the results from FT-IR. Fig. 3c displays the high-resolution XPS spectra of C 1s, which can be deconvoluted into three peaks, corresponding to the C=C (284.4 eV), C-O/C-N (285.4 eV) and C=O (287.6 eV), respectively [41]. The in-

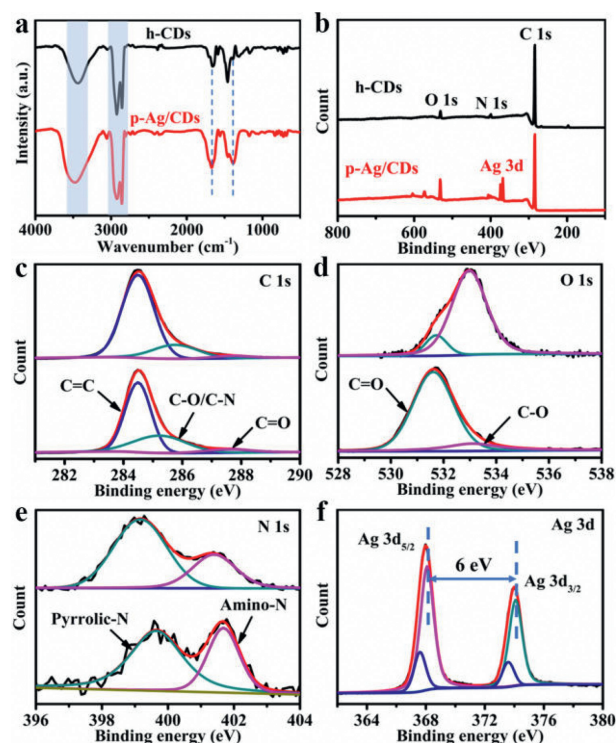


**Fig. 3.** (a) FT-IR spectra of h-CDs and p-Ag/CDs, respectively. (b) XPS survey scan of h-CDs and p-Ag/CDs. (c-f) High-resolution XPS spectra of h-CDs and p-Ag/CDs: (c) C 1s, (d) O 1s, (e) N 1s, (f) Ag 3d.

creased content of C-O/C-N and C=O groups in p-Ag/CDs compared to h-CDs (Table S2 in Supporting information) may result in the FL blue shift of p-Ag/CDs [43]. Fig. 3d shows the high-resolution O 1s spectra of h-CDs and p-Ag/CDs. Two fitted peaks at 531.6 eV and 533.1 eV can be assigned to the C=O and C-O groups, respectively [44]. The content of C=O groups in p-Ag/CDs (87.2%) is much higher than that in h-CDs (12.6%), further demonstrating that there are more O-contained groups in p-Ag/CDs, which is consistent with the FT-IR results. The high-resolution N 1s band (Fig. 3e) of h-CDs contains two peaks of 399.1 eV and 401.4 eV, which are pyrrolic-N and amino-N, respectively [30]. But for p-Ag/CDs, these two peaks shift to higher binding energy at 399.7 eV and 401.7 eV respectively, indicating the interaction between CDs and AgNPs by Ag-N bond through the coordination of Ag with N atom [45]. The chemical state of Ag in p-Ag/CDs was investigated from its high-resolution XPS spectrum (Fig. 3f). The binding energy of Ag 3d can be presented as two pairs of peaks. The first pair with spin-orbit splitting energy of 6.0 eV at 374.1 eV (Ag 3d<sub>3/2A</sub>) and 368.1 eV (Ag 3d<sub>5/2A</sub>) can be assigned as the metallic silver (Ag<sup>0</sup>), indicating the formation of AgNPs under the continuous UV light irradiation. The second pair at 373.5 eV (Ag 3d<sub>3/2B</sub>) and 367.5 eV (Ag 3d<sub>5/2B</sub>) suggests a pronounced ionic state, indicating the co-existed Ag<sup>+</sup> and Ag<sup>0</sup> in p-Ag/CDs [46].

To explore the exact effects of UV irradiation and silver on the optical properties of p-Ag/CDs, several related materials are also prepared and characterized, such as the UV irradiated h-CDs (CDs-hν), simply physical mixed Ag<sup>+</sup> and CDs-hν (Ag<sup>+</sup>/CDs-hν). Fig. 4a shows the FL spectra of h-CDs before and after UV irradiation (CDs-hν) without Ag<sup>+</sup>. One can see that the CDs-hν also exhibits a distinct blue shift FL emission with a visible FL ranging from yellow to blue (Insets of Fig. 4a). However, the FL intensity is not affected after the UV irradiation (Fig. 4a). The XPS of CDs-hν was also tested to investigate the effect of UV irradiation on the surface groups of h-CDs. The results (Fig. S6 and Table S3 in Supporting information) also turn out that UV irradiation can cause the increase

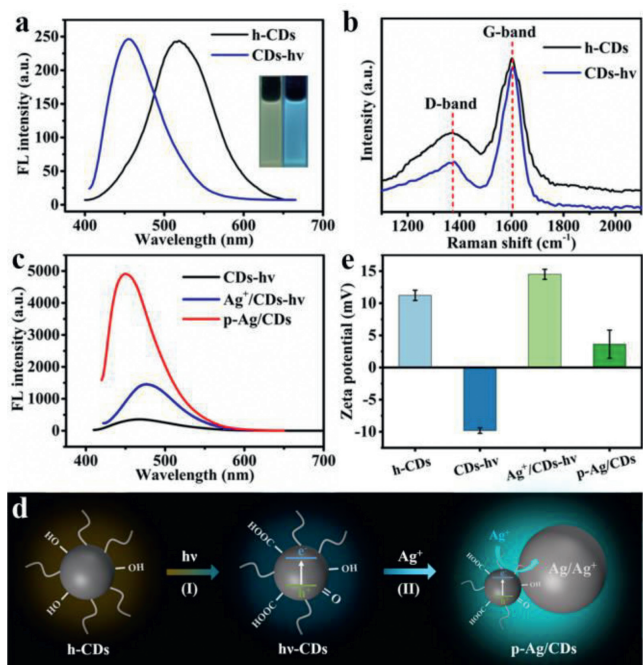


**Fig. 4.** (a) FL emission spectra of h-CDs and CDs-hv. (b) Raman spectra of h-CDs and CDs-hv. (c) FL emission spectra of CDs-hv, Ag<sup>+</sup>/CDs-hv and p-Ag/CDs. (d) Schematic diagram of FL enhancement mechanism of h-CDs under ultraviolet irradiation. (e) Zeta potential of h-CDs, CDs-hv, Ag<sup>+</sup>/CDs-hv and p-Ag/CDs.

of O-contained groups on CDs, which is consistent with the results obtained from p-Ag/CDs (Fig. 3b). Fig. 4b displays the Raman spectra of h-CDs before and after UV irradiation (CDs-hv), where the D band (1367 cm<sup>-1</sup>) and G band (1604 cm<sup>-1</sup>) correspond to the disordered and graphitic structures of carbon material. The lower  $I_D/I_G$  of CDs-hv (0.29) than that of h-CDs (0.44) suggests that UV irradiation can lead to the formation of the graphitic structure of CDs-hv, which is closely related to its FL blue shift [41]. All these results indicate that UV irradiation can increase the O-contained groups and graphitic structure of h-CDs, which leads to the blue shift of FL emission. However, UV irradiation cannot result in the FL enhancement of h-CDs.

Furthermore, the FL spectra of CDs-hv and Ag<sup>+</sup>/CDs-hv were tested to investigate the effect of Ag<sup>+</sup> on the optical property of CDs. Fig. 4c displays the FL spectra of CDs-hv, Ag<sup>+</sup>/CDs-hv and p-Ag/CDs, respectively. We can see that the FL intensity of Ag<sup>+</sup>/CDs-hv is stronger than CDs-hv but much weaker than p-Ag/CDs, which should also be caused by the formation of AgNPs in solution, as evidenced by the small shoulder absorption peak around 400 nm after the addition of Ag<sup>+</sup> to CDs-hv (Fig. S7 in Supporting information). It has been demonstrated that metal nanoparticles (MNPs) can enhance the FL by the coupling of plasma to proximal fluorophores, known as metal-enhanced fluorescence (MEF) [47]. In this work, the SPR adsorption of formed AgNPs (400 nm) completely overlaps with the excitation wavelength of h-CDs (400 nm). Therefore, the electric field generated near the surface of AgNPs with photoexcitation can greatly enhance the FL intensity of h-CDs. To prove the stronger FL of p-Ag/CDs belongs to MEF, nitric acid was added to the p-Ag/CDs solution, which can dissolve the generated AgNPs. The result (Fig. S8 in Supporting information) shows that the FL intensity (460 nm) of the system is greatly decreased after the removal of AgNPs. These results indicate that the greatly enhanced FL of h-CDs is due to the surface resonance effect of AgNPs.

Based on the above results, we can conclude that UV irradiation and generated AgNPs play an indispensable role in the outstanding

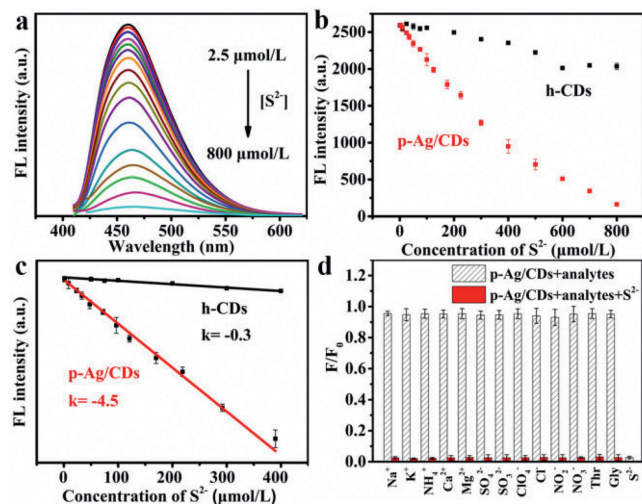


**Fig. 5.** (a) FL spectra of p-Ag/CDs (0.5 mg/mL) upon the titration of S<sup>2-</sup> (2.5–800 μmol/L). (b) Plots of the FL intensity (460 nm) of p-Ag/CDs and h-CDs versus the concentration of S<sup>2-</sup> (2.5–800 μmol/L). (c) Linear correlation of FL intensity of p-Ag/CDs and h-CDs toward S<sup>2-</sup> (2.5–400 μmol/L). (d) Effects of various interferences (800 μmol/L) on the FL intensity of p-Ag/CDs with the absence/co-existence of S<sup>2-</sup> (800 μmol/L).

optical properties of p-Ag/CDs. With the UV irradiation, photogenerated carriers (h<sup>+</sup>-e<sup>-</sup>) are generated on h-CDs (Fig. 4d). The strong oxidability of h<sup>+</sup> can lead to the increase of O-contained groups (-OH and/or -COOH) on h-CDs (Fig. 4d, I), which can not only result in a blue shift FL of h-CDs but also facilitate the adsorption of Ag<sup>+</sup> on its surface. At the same time, the adsorbed Ag<sup>+</sup> is reduced to AgNPs by the photogenerated electrons (e<sup>-</sup>) (Fig. 4d, II), and the SPR effect of AgNPs greatly increases the FL intensity of h-CDs. These processes can also be further demonstrated by the measured zeta potential (pH 7) of several materials (Fig. 4e), including h-CDs, CDs-hv, Ag<sup>+</sup>/CDs-hv and p-Ag/CDs. It can be seen that the h-CDs are positively charged with a zeta potential of 11.2 mV. After the UV irradiation, the zeta potential of CDs-hv changes to -9.8 mV, attributing to the increased -OH and/or -COOH on CDs-hv during this irradiation process, which has been proved by the XPS results (Table S3) and FT-IR. Furthermore, the Ag<sup>+</sup> in the solution can be easily adsorbed on this negatively charged CDs-hv based on the electrostatic effect [39], and lead to a positive zeta potential of Ag<sup>+</sup>/CDs-hv (14.5 mV) again. With the irradiation of UV light, parts of the adsorbed Ag<sup>+</sup> can be reduced to Ag<sup>0</sup> on h-CDs by the photogenerated electrons, and formed p-Ag/CDs possess a lower positive zeta potential (3.6 mV). Interestingly, the p-Au/CDs prepared with the same method also exhibit an enhanced FL emission (Fig. S9 in Supporting information), indicating the universality of this method to enhance the FL property of h-CDs based on noble metals (Au, Ag).

The greatly enhanced FL of p-Ag/CDs will undoubtedly broaden its application in the fields of sensing. It is well known that Ag-contained materials usually exhibit a good response to S<sup>2-</sup>, a common pollutant in the environment. Therefore, we investigated the FL response of h-CDs and p-Ag/CDs to S<sup>2-</sup> in this work. As illustrated in Fig. 5a, the FL intensity (460 nm) of p-Ag/CDs decreases significantly with the increased concentration of S<sup>2-</sup>, which cannot lead to an obvious effect on the FL intensity of h-CDs (Fig. S10 in Supporting information). The FL quenching of p-Ag/CDs should be attributed to the interaction between Ag/Ag<sup>+</sup> and S<sup>2-</sup>. This result indicates that the modulation of Ag not only greatly enhances the FL properties of CDs, but also endows CDs with a derivative sensing function toward S<sup>2-</sup>. Fig. 5b shows the FL intensity (460 nm) of p-Ag/CDs and h-CDs as a function of S<sup>2-</sup> concentrations rang-

**Table 1**

Detection of  $S^{2-}$  in the samples of lotus pond water, soil and white sugar based on the constructed p-Ag/CDs probe.

Sample	$S^{2-}$ added ( $\mu\text{mol/L}$ )	$S^{2-}$ found ( $\mu\text{mol/L}$ )	Recovery ( $n=3$ , %)	RSD ( $n=3$ , %)
Lotus pond water	5	4.74 $\pm$ 0.13	95.09	2.72
	50	49.15 $\pm$ 1.11	98.29	2.25
	200	198.03 $\pm$ 6.00	99.01	3.03
Soil	5	4.91 $\pm$ 0.13	98.09	2.64
	50	49.22 $\pm$ 1.62	98.45	3.28
	200	200.79 $\pm$ 4.66	100.39	2.32
White sugar	5	5.21 $\pm$ 0.13	104.07	2.49
	50	51.24 $\pm$ 1.78	102.48	3.47
	200	199.45 $\pm$ 6.84	99.72	3.43

ing from 2.5  $\mu\text{mol/L}$  to 800  $\mu\text{mol/L}$ , respectively. From the results, it is obvious that the response of p-Ag/CDs to  $S^{2-}$  is more sensitive than that of h-CDs. Moreover, an excellent linear relationship between the FL intensity of p-Ag/CDs and the concentration of  $S^{2-}$  from 2.5  $\mu\text{mol/L}$  to 400  $\mu\text{mol/L}$  can be obtained (Fig. 5c) and expressed as  $F=2604.5-4.5[S^{2-}]$  ( $R^2=0.997$ ), and the response sensitivity of p-Ag/CDs to  $S^{2-}$  is 12.6 times higher than that of h-CDs ( $F=1423.8-0.3[S^{2-}]$ ,  $R^2=0.984$ ). The limit of detection (LOD) of p-Ag/CDs toward  $S^{2-}$  can be calculated as 0.11  $\mu\text{mol/L}$  ( $S/N=3$ ), which is well below the World Health Organization (WHO) allowable limit for  $S^{2-}$  (15  $\mu\text{mol/L}$ ) in drinking water. In addition, this work also offers superior performance (higher sensitivity, wider linear response and lower LOD) for the detection of  $S^{2-}$  compared with most other reported FL probes (Table S4 in Supporting information). The selectivity of the p-Ag/CDs probe towards  $S^{2-}$  was studied according to the changes in the FL spectra of p-Ag/CDs with the presence of common interferences, including  $\text{Na}^+$ ,  $\text{K}^+$ ,  $\text{NH}_4^+$ ,  $\text{Ca}^{2+}$ ,  $\text{Mg}^{2+}$ ,  $\text{SO}_4^{2-}$ ,  $\text{SO}_3^{2-}$ ,  $\text{ClO}_4^-$ ,  $\text{Cl}^-$ ,  $\text{NO}_2^-$ ,  $\text{NO}_3^-$ , L-threonine and glycine. As shown in Fig. 5d, we can conclude that these coexisting interferences cannot cause any significant influence, indicating the proposed method possesses higher specificity and anti-interference ability for  $S^{2-}$  detection. In addition, the reproducibility of constructed p-Ag/CDs fluorescent probe was investigated by measuring five samples with  $S^{2-}$  (100  $\mu\text{mol/L}$ ), and a relative standard deviation (RSD) of 4.77% can be obtained, indicating its good reproducibility for  $S^{2-}$  detection. To further evaluate the feasibility of constructed FL probes based on p-Ag/CDs in practical analysis, it was employed to measure the  $S^{2-}$  in three kinds of samples, including the lotus pond water, soil and white sugar. In addition, the recovery test was also conducted to demonstrate its accuracy. From the obtained results (Table 1), the satisfactory recovery (95.09%–104.07%) and lower RSD (2.25%–3.47%) demonstrate that our proposed FL probe offers an excellent and accurate method for  $S^{2-}$  analysis, which can be applied to the detection in complex real samples.

In summary, we developed a novel strategy based on photo-induced Ag modulating to greatly enhance the FL property of h-CDs by irradiation of the mixed solution of h-CDs and  $\text{Ag}^+$  with UV light. The QY of obtained p-Ag/CDs can be improved to 51.1%, which is much higher than that of the original of h-CDs (4.9%). In addition, a blue shift of FL emission for p-Ag/CDs compared to h-CDs is also generated in this UV irradiation process. The mechanism for FL enhancement and blue shift of p-Ag/CDs is also studied, and the results demonstrate that it is the increased O-contained groups by UV irradiation that lead to the FL blue-shift of h-CDs, and the AgNPs generated in this process results in the greatly enhanced FL intensity based on MEF. More interesting is that the Ag modulating endows p-Ag/CDs with newly derived sensing response to  $S^{2-}$ , which has been successfully used to construct an FL probe for  $S^{2-}$  detection in real complex samples with higher sensitivity and selectivity. This work provides a new strategy not only to improve the FL properties of CDs but also to endow CDs

with new derived functions, which will expand its new applications in many fields.

### Declaration of competing interest

The authors declare that they have no known competing financial interests or personal relationships that could have appeared to influence the work reported in this paper.

### Acknowledgments

This work is financially supported by the National Natural Science Foundation of China (Nos. U1833202 and 21876117), and the Open Research Fund of the School of Chemistry and Chemical Engineering, Henan Normal University (No. 2021YB05).

### Supplementary materials

Supplementary material associated with this article can be found, in the online version, at doi:10.1016/j.ccllet.2023.108277.

### References

- [1] X. Xu, R. Ray, Y. Gu, et al., *J. Am. Chem. Soc.* 126 (2004) 12736–12737.
- [2] S. Li, L. Li, H. Tu, et al., *Mater. Today* 51 (2021) 188–207.
- [3] D.S. Achilleos, H. Kasap, E. Reisner, *Green Chem.* 22 (2020) 2831–2839.
- [4] Z. Zhao, S. Reischauer, B. Pieber, M. Delbianco, *Green Chem.* 23 (2021) 4524–4530.
- [5] Y. Wang, B.B. Chen, Y.T. Gao, et al., *J. Colloid Interface Sci.* 606 (2022) 600–606.
- [6] Y. Liu, X. Li, Q. Zhang, et al., *Angew. Chem. Int. Ed.* 59 (2020) 1718–1726.
- [7] L. Li, L. Shi, J. Jia, et al., *ACS Appl. Mater. Interfaces* 12 (2020) 18250–18257.
- [8] X. Zhang, X. Tan, Y. Hu, *J. Hazard. Mater.* 411 (2021) 125184.
- [9] Y. Ma, A.Y. Chen, Y.Y. Huang, et al., *Carbon* 162 (2020) 234–244.
- [10] M. Wang, R. Shi, M. Gao, et al., *Food Chem.* 318 (2020) 126506.
- [11] X. Li, X. Xing, S. Zhao, et al., *Chin. Chem. Lett.* 33 (2022) 1632–1636.
- [12] R. Guo, T. Li, S. Shi, *J. Mater. Chem. C* 7 (2019) 5148–5154.
- [13] X. Wang, X. Zhang, X. Gu, et al., *Adv. Opt. Mater.* 8 (2020) 2000239.
- [14] F. Yuan, Y.K. Wang, G. Sharma, et al., *Nat. Photon.* 14 (2020) 171–176.
- [15] L. Wang, W. Li, L. Yin, et al., *Sci. Adv.* 6 (2020) eabb6772.
- [16] Y. Li, Q. Li, S. Meng, et al., *Chin. Chem. Lett.* 34 (2023) 107794.
- [17] B.B. Karakoçak, A. Laradji, T. Primeau, et al., *ACS Appl. Mater. Interfaces* 13 (2021) 277–286.
- [18] Z.M. Marković, M. Labudová, M. Danko, et al., *ACS Sustain. Chem. Eng.* 8 (2020) 16327–16338.
- [19] M. Choppadandi, A.T. Guduru, P. Gondaliya, et al., *Mater. Sci. Eng. C* 129 (2021) 112366.
- [20] G. Zou, S. Chen, N. Liu, Y. Yu, *Chin. Chem. Lett.* 33 (2022) 778–782.
- [21] T.T. Meiling, R. Schürmann, S. Vogel, et al., *J. Phys. Chem. C* 122 (2018) 10217–10230.
- [22] X. Yang, X. Li, B. Wang, et al., *Chin. Chem. Lett.* 33 (2022) 613–625.
- [23] Y.P. Sun, B. Zhou, Y. Lin, et al., *J. Am. Chem. Soc.* 128 (2006) 7756–7757.
- [24] H. Luo, N. Papaioannou, E. Salvadori, et al., *ChemSusChem* 12 (2019) 4432–4441.
- [25] T. Li, W. Shi, E. Shuang, Q. Mao, X. Chen, *J. Colloid Interface Sci.* 591 (2021) 334–342.
- [26] S. Zhao, X. Chen, C. Zhang, et al., *ACS Appl. Mater. Interfaces* 12 (2021) 61565–61577.
- [27] L. Wang, B. Wang, E. Liu, et al., *Chin. Chem. Lett.* 33 (2022) 4111–4115.
- [28] J. Manioudakis, F. Victoria, C.A. Thompson, et al., *J. Mater. Chem. C* 7 (2019) 853–862.
- [29] Y. Wei, L. Chen, S. Zhao, et al., *Front. Mater. Sci.* 15 (2021) 253–265.
- [30] L. Jiang, H. Ding, S. Lu, et al., *Angew. Chem. Int. Ed.* 59 (2020) 9986–9991.
- [31] X.Y. Zhang, Y. Li, Y.Y. Wang, et al., *J. Colloid Interface Sci.* 611 (2022) 255–264.
- [32] Y. Wu, D. Qin, Z. Luo, et al., *ACS Sustain. Chem. Eng.* 10 (2022) 5195–5202.
- [33] N. Soni, S. Singh, S. Sharma, et al., *Chem. Sci.* 12 (2021) 3615–3626.
- [34] M.K. Meher, K.M. Poluri, *Carbohydr. Polym.* 266 (2021) 118124.
- [35] K. Arkin, Y. Zheng, J. Hao, S. Zhang, Q. Shang, *ACS Appl. Nano Mater.* 4 (2021) 8500–8510.
- [36] Z. Zhang, F. Xi, Q. Ma, et al., *Mater. Today Nano* 17 (2022) 100162.
- [37] F. Wei, X. Zhao, C. Li, X. Han, *Sci. Pollut. Res.* 25 (2018) 19480–19487.
- [38] B. Wang, Z. Wei, L. Sui, et al., *Light Sci. Appl.* 11 (2022) 172.
- [39] T. Gao, X. Wang, L.Y. Yang, et al., *ACS Appl. Mater. Interfaces* 9 (2017) 24846–24856.
- [40] Q. Wang, Y. Gao, B. Wang, et al., *J. Mater. Chem. C* 8 (2020) 4343–4349.
- [41] H. Ding, S.B. Yu, J.S. Wei, H.M. Xiong, *ACS Nano* 10 (2016) 484–491.
- [42] Z. Mu, J. Tian, J. Wang, J. Zhou, L. Bai, *Appl. Surf. Sci.* 573 (2022) 151601.
- [43] B. Wang, J. Yu, L. Sui, et al., *Adv. Sci.* 8 (2021) 2001453.
- [44] X. Yang, L. Ai, J. Yu, et al., *Sci. Bull.* 67 (2022) 1450–1457.
- [45] S. Zhang, Z. Mo, J. Wang, et al., *Electrochim. Acta* 390 (2021) 138831.
- [46] M. Zienkiewicz-Strzałka, A. Deryło-Marczewska, *Int. J. Mol. Sci.* 21 (2020) 9388.
- [47] W. Yang, G. Zhang, J. Ni, Z. Lin, *Microchim. Acta* 187 (2020) 137.